Jurnal Ilmiah Teknik Elektro Komputer dan Informatika (JITEKI)
Vol. 10, No. 2, June 2024, pp. 302-312
ISSN: 2338-3070, DOI: 10.26555/jiteki.v10i2.28797

Dual Mode MIMO-Beamforming Four Elements Array Antenna for Mobile Robot Communications at 5.6 GHz

Muhsin[1,2], Aulia Saharani[1,3], Afina Lina Nurlaili[4]
[1]School of Electrical Engineering, Telkom University, Surabaya 60231, Indonesia
[2]University Center of Excellence for Intelligent Sensing-IoT, Telkom University, Bandung 40257, Indonesia
[3]Department of Electrical Engineering, Institut Teknologi Sepuluh Nopember, Surabaya 60111, Indonesia
[4]Department of Informatics, Universitas Pembangunan Nasional "Veteran" Jawa Timur, Surabaya 60294, Indonesia

ARTICLE INFO

Article history:

Received May 09, 2024
Revised June 29, 2024
Published July 03, 2024

Keywords:

Antenna;
Array;
MIMO;
Beamforming;
Robot communications

ABSTRACT

Mobile robot communications are essential for robot teamwork. To enable communication between robots, reliable wireless communications must be deployed. Higher performance and capacity for communication are required. Multiple-input multiple-output (MIMO) and beamforming are important wireless communication technologies that use multiple antennas to improve communications performance and capacity. However, these two technologies have different requirements. MIMO requires the antenna element to be independent. While beamforming needs antennas to be coupled and fed by the same source. This paper proposes a dual-mode antenna for mobile robot communications at 5.6 GHz that supports both beamforming and MIMO. A single antenna consists of a planar dipole antenna arranged in a circular configuration. This antenna is then expanded to a four-element array antenna. Both MIMO and beamforming evaluations are performed. In MIMO mode, the bit error rate (BER) performance is very similar to a non-correlated MIMO antenna. The BER of 10^{-3} is achieved at SNR of 16dB with quadrature-phase shift keying (QPSK) modulation and quasi-orthogonal space time block codes. It is supported by the very low correlation between antennas below 0.01. Low coupling is also achieved below -16.5 dB. In beamforming mode, the proposed antenna achieves more than 8.6 dBi gain and good beam steering capability. It is supported by beam suppression with a 90° phase difference between the front and back direction. The proposed antenna performs well in both the MIMO and beamforming modes.

Corresponding Author:

M. Muhsin, School of Electrical Engineering, Telkom University, Surabaya 60231, Indonesia
Email: mmuhsin@telkomuniversity.ac.id

1. INTRODUCTION

In the era of widespread robot use, effective communication between robots is critical. As robots become more integrated into various applications, seamless interaction and coordination among them become essential [1]–[7]. Robot communication enables tasks that require collaboration, synchronization, and shared understanding, increasing efficiency and productivity across industries. Robust communication systems enable robots to work together to achieve common goals. These goals include autonomous smart agriculture, rescue operation, logistics, and surveillance. More applications are also possible. Furthermore, effective communication ensures safety, eliminates errors, and streamlines operations, ultimately contributing to the advancement and integration of robotic technologies into society.

Radio-based communication provides robust and flexible communication between robots. A wireless local area network (WLAN) is the most common technology for allowing robots to communicate in a limited area [8]–[12]. As for WLAN, there are two most frequently used frequencies [13]–[16]. The low frequency 2.4 GHz may provide wide coverage of area. However, the capacity is limited. Another frequency is 5.6 GHz

which has a higher capacity compared to 2.4 GHz with limited coverage. In this case, 5.6 GHz is more suitable for high-density networks of robots.

In modern wireless communications, multiple antennas are used. There are two applications for multiple antennas. Multiple-input multiple-output (MIMO) technology uses multiple antennas to provide diversity [17]–[20]. As a result, efficiency and capacity can be improved. While beamforming uses multiple antennas to direct radiation patterns in a specific direction [21]–[25]. It increases coverage by suppressing radiation patterns in other unwanted directions. These techniques of multiple antennas are applicable for WLAN, including for robot communications.

Diversity is the key aspect of the MIMO antenna's design. In this case, each antenna should work independently. Therefore, a low correlation between antennas is expected [26]–[32]. In contrast, a beamforming antenna requires all antennas to work together from a single feeding point. However, the signal is principally similar since a single feeding point is applied. Therefore, correlation is maximum between elements.

There are several techniques used to minimize the correlation between antennas for MIMO. Traditionally, the antenna should be spaced by half-wavelength or other spacing rules [33]–[38]. Additionally, decoupling structures can be used to reduce the spacing of antennas [39]–[44]. Moreover, dual-polarization or cross-polarization between neighboring antennas also can reduce correlations [45]–[50].

Beamforming antennas are commonly used for adaptive radiation patterns. In this case, radiation patterns will follow the specific object [51]–[55]. A phased array is frequently used to achieve this feature. Each element is varied by amplitude and phase [56]–[60]. Moreover, some algorithms can be used to detect the position of a specific object and apply beamforming parameters to that object [61]–[64].

For mobile robot applications, both MIMO and beamforming are very useful. However, both features may require different designs. In this research, a dual-mode four-element dipole array is proposed. The antenna array is suitable for both MIMO and beamforming applications. Specific arrangements of antennas are employed to achieve this feature. A frequency of 5.6 GHz is chosen for high-density network applications following the trend of massive Internet of Things (IoT).

In this research, a simple array antenna design is proposed. The array antenna design is set by phase configuration to achieve good beamforming ability. Moreover, the design has good isolation between elements to work on the MIMO scenario. Therefore, a dual-mode array antenna that is suitable for both beamforming and MIMO is presented.

2. ANTENNA DESIGN

Research flow is presented in Fig. 1. To design the dual-mode array antenna, a single antenna is constructed and expanded into a four-element array antenna. Subsection 2.1 describes the design of a single antenna. Subsection 2.2 explains the array antenna. Subsection 2.2 explains the MIMO system. Subsection 2.3 explains the beamforming system. Finally, Section 3 explains the evaluation of MIMO and beamforming performance.

2.1. Single Antenna

A four-element antenna begins with a single antenna. A planar dipole antenna was chosen for the present research due to its simple design and radiation pattern. A dipole antenna has an omnidirectional radiation pattern, making it easy to create a beamforming antenna. It also has roughly the same uniform radiation power in the azimuth plane. This dipole antenna is then made planar. Planar antennas offer some advantages, such as ease of manufacture and reduced manufacturing error.

A planar dipole antenna is a dipole antenna that is made in a planar shape, similar to a printed circuit board (PCB) as shown in Fig. 2. PCB material is essential to achieving optimal performance. Each material has its own fundamental properties, such as permittivity, permeability, and conductivity. These parameters determine the material's characteristics. It is important to choose the appropriate material.

Rogers RT-5880 was selected as the PCB material for this research. This material has a relative permittivity of ε_r=2.2, making it suitable for lower lossy characteristics, particularly when compared to FR4 [65]. Lower permittivity also increased the antenna size and reduced the antenna's printing error. Because of its regularity, the substrate height of h=1.6 mm was chosen for this antenna design. This regularity makes it simple to find and manufacture. Simplified formula of dipole antenna is used as

$$l = \frac{143}{f_{\text{MHz}}} \quad (1)$$

where l is dipole length in meters, f_{MHz} is the antenna's resonance frequency in megahertz (MHz), and the reference impedance is 50 Ohm. The antenna is then optimized to get proper performance by changing the antenna dimension.

Table 1 displays the variables for the optimized dimension. This optimization process focuses on the antenna's reflection coefficient. The obtained return loss is presented in Fig. 3. The antenna has a bandwidth of 1.37 GHz and a working frequency range of 4.8238 GHz to 6.1938 GHz, which meets the WLAN 5.6 GHz requirement of 5.15 GHz to 5.85 GHz.

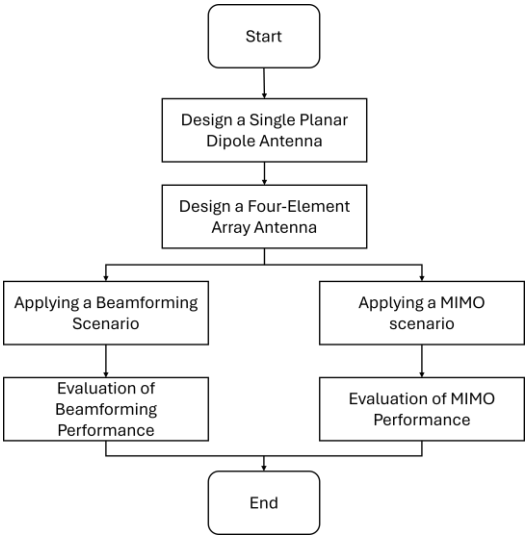

Fig. 1. Research Flow

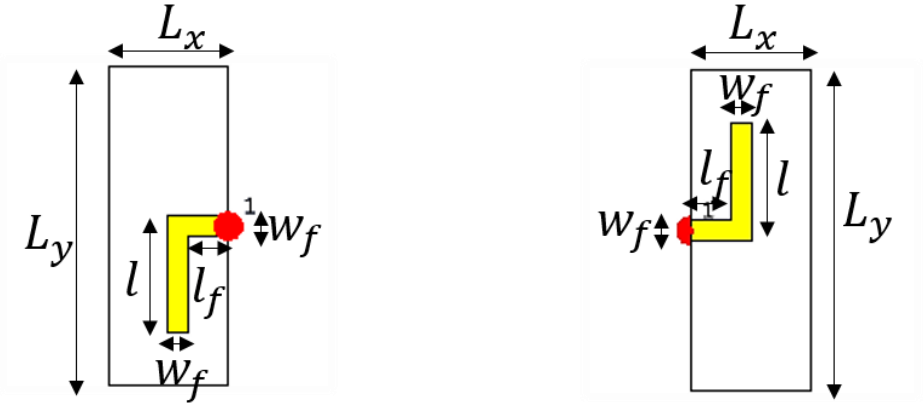

(a) (b)

Fig. 2. Planar dipole antenna

Table 1. Optimized Dimension of Planar Dipole Antenna

Variable	Value
w_f	2.7 mm
l_f	5 mm
l	12 mm
L_x	15 mm
L_y	40 mm

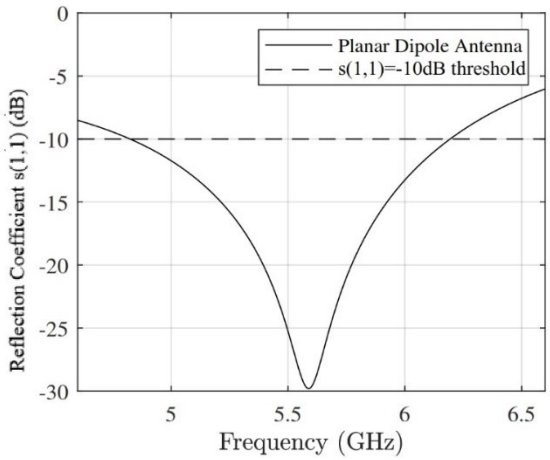

Fig. 3. Reflection coefficient of planar dipole antenna

Fig. 4 shows the obtained radiation pattern of a single antenna. The single planar dipole antenna has an omnidirectional radiation pattern in the xz-plane azimuth direction and a gain of 2.416 dBi. It means that the antenna produces the same uniform radiation power in all directions on the azimuth or xz plane. This radiation pattern confirms that the antenna met the requirements and can be used in the next step of the array antenna design.

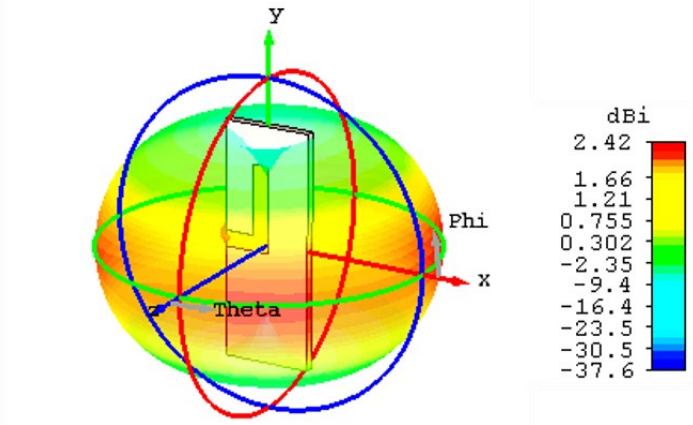

Fig. 4. Radiation pattern of planar dipole antenna

2.2. Array Antenna

Fig. 5 illustrates an array antenna made up of four single antennas. Four dipole antennas are arranged in a circular azimuth pattern. It enables radiation pattern control on azimuth planes. Due to limited space, the antenna is fed from the outside. The circle has a radius of r=30 mm. This radius was chosen as the most rational spacing for effective coupling reduction.

Coupling is an important parameter in array antenna design. Antenna coupling is the interaction of antennas that are close to each other or share a common medium. This interaction can occur via a variety of mechanisms, including electromagnetic fields, physical proximity, and electrical connections. In Fig. 6, the non-diagonal element of the antenna's s-parameter matrix represents the coupling as

$$S = \begin{pmatrix} S_{1,1} & S_{1,2} & S_{1,3} & S_{1,4} \\ S_{2,1} & S_{2,2} & S_{3,3} & S_{2,4} \\ S_{3,1} & S_{3,2} & S_{3,3} & S_{3,4} \\ S_{4,1} & S_{4,2} & S_{4,3} & S_{4,4} \end{pmatrix} \quad (2)$$

where each $s_{i,j}$ is coupling between antenna i and j. Fig. 5 shows the obtained coupling of the four-element array antenna. The antenna has a coupling of -19.5 dB to -16.5 dB at 5.15-5.85 GHz.

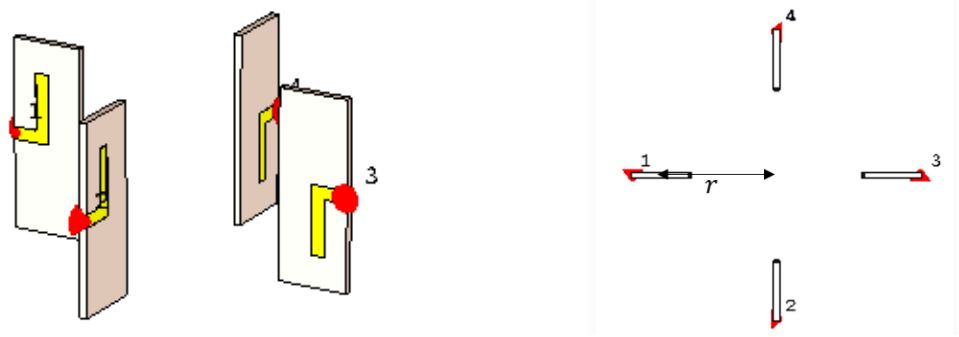

(a) (b)

Fig. 5. Array antenna design: (a) 3-dimensional view, (b) xz plane view

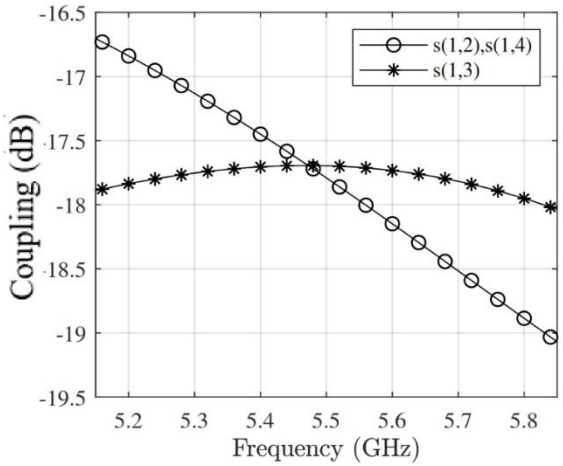

Fig. 6. Reflection coefficient of planar dipole antenna

2.3. MIMO Systems

MIMO systems perform by applying MIMO coding to transmitting antennas. Fig. 7 shows the simulation model for MIMO systems used in this research. The received signal is

$$\mathbf{y} = \mathbf{H}\mathbf{x} + \mathbf{n} \tag{3}$$

where $\mathbf{y}$ is the signal at the receiver, $\mathbf{H}$ is the $N_r \times N_t$ channel matrix, $\mathbf{x}$ is the signal at the transmitter, and $\mathbf{n}$ is the additive white Gaussian noise vector. N_t is the number of antennas at the transmitter, while N_r is the number of antennas at the receiver. Extended-Alamouti quasi-orthogonal space-time block codes (QOSTBC) are utilized. In this research, the four transmit bits x_1, x_2, x_3, x_4 are encoded as [49], [66].

$$C_{EA4} = \begin{pmatrix} x_1 & x_2 & x_3 & x_4 \\ -x_2^* & x_1^* & -x_4^* & x_3^* \\ -x_3^* & -x_4^* & x_1^* & x_2^* \\ x_4 & -x_3 & -x_2 & x_1 \end{pmatrix}. \tag{4}$$

$\mathbf{H}$ in (3) typically represents a fully independent MIMO channel. To generate a channel matrix for correlated MIMO channels, use the Kronecker model [67].

$$\mathbf{H} = \mathbf{R}_r^{\frac{1}{2}} \times \mathbf{H}_{i.i.d} \times \mathbf{R}_t^{\frac{1}{2}} \tag{5}$$

where $R_r^{\frac{1}{2}}$ is the receiver's correlation matrix, $\mathbf{H}_{i.i.d}$ is the physically independent and identically distributed MIMO channel matrix, and $\mathbf{R}_t^{\frac{1}{2}}$ is the transmitter's correlation matrix. The maximum ratio combiner (MRC) is used for MIMO decoding.

To simplify the simulation, MRC is applied using an equivalent virtual channel matrix (EVCM). The received signal vector is formed from the conventional received signal in (3) as [49], [68], [69].

$$\mathbf{y}_{eq} = \mathbf{C}_h\mathbf{x} + \mathbf{v} \tag{6}$$

where C_h is a $N_c \times N_t$ coded channel matrix using EA-QOSTBC, $\mathbf{h} = [h_1 \quad h_2 \quad h_3 \quad \dots \quad h_{N_c}]^{\mathrm{T}}$ is an i.i.d Rayleigh fading channel element, $\mathbf{x}$ is an uncoded transmit signal $\mathbf{x} = [x_1 \quad x_2 \quad x_3 \quad \dots \quad x_{N_t}]^{\mathrm{T}}$, and $N_c = 4$. Based on (5), MRC can be expressed as

$$\hat{\mathbf{x}} = \left(\mathbf{C}_h\mathbf{C}_h^{\mathrm{H}}\right)^{-1}\mathbf{C}_h^{\mathrm{H}}\mathbf{y} \tag{7}$$

where $\mathbf{C}_h^H$ represents the Hermitian transpose of $\mathbf{C}_h$.

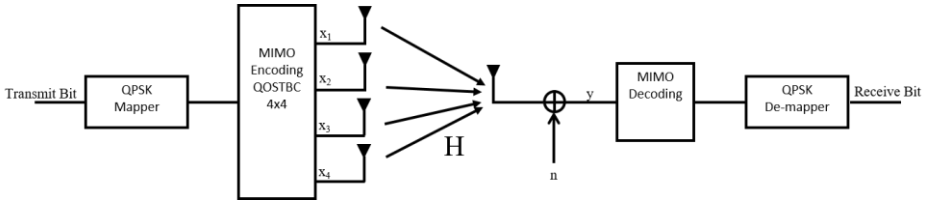

Fig. 7. A 4×1 MIMO scheme using 4×4 QOSTBC

2.4. Beamforming Systems

Array antennas can be used in beamforming applications. In this scenario, each antenna gets the same signal source with varying magnitude and phase, as illustrated in Fig. 8. The combined radiation pattern for an array of isotropic antennas is

$$U_{\text{tot}} = \sum_{i=1}^{n} W_i e^{j\theta_i} \tag{8}$$

where W_i is the power amplitude, j is $\sqrt{-1}$, and θ_i is the initial phase. By adjusting the magnitude and phase of the antenna, electromagnetic waves will interfere with one another, producing maximal and minimal results in specific directions.

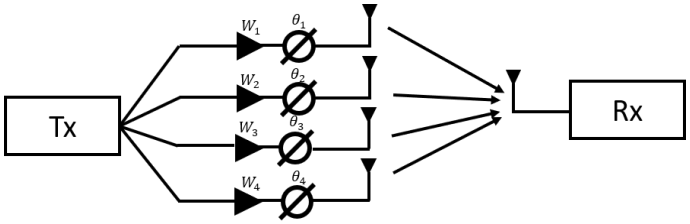

Fig. 8. Beamforming scheme

3. RESULTS AND DISCUSSION

In this section, the results of the research are explained and, at the same time is given a comprehensive discussion. Results can be presented in figures, graphs, tables, and others that make the reader understand easily. The discussion can be made in several sub-chapters. It is strongly suggested that comparison wih results from other published articles are provided to give more context and to strengthen the claim of novelty.

3.1. MIMO Performance

The MIMO performance of the designed antenna is evaluated using the system shown in Fig. 7. The proposed antenna's bit error rate (BER) is compared to one that is not correlated. Fig. 9 shows the BER performance of the proposed antenna. The proposed antenna's BER performance is similar to that of a non-correlated antenna. The proposed antenna's good BER performance indicates there is a low correlation between antennas. To calculate the envelope correlation coefficient (ECC), use the antenna's s-parameter as [50], [70], [71].

$$\rho_{i,j} = \frac{\left|s_{i,i}^{*}s_{i,j}\right|^2}{\left(1-\left(\left|s_{i,i}\right|^2+\left|s_{j,i}\right|^2\right)\right)\left(1-\left(\left|s_{j,j}\right|^2+\left|s_{i,j}\right|^2\right)\right)} \tag{9}$$

where i and j represent the antenna's index with $i \neq j$. The ideal ECC value is zero, which indicates no correlation between antennas.

The ECC of the proposed antenna is shown in Fig. 10. The low correlation between antennas results in a very low ECC. The proposed antenna's excellent BER performance is primarily due to its extremely low ECC. The proposed antenna's BER has less diversity than 4. Ideally, a MIMO system with four transmit antennas and one receive antenna can provide a diversity order of four. In this paper, QOSTBC in (2) limits the diversity order due to the lack of orthogonality in MIMO coding. The orthogonality of QOSTBC can be approximated by [69].

$$\kappa = \frac{1}{2} + \frac{1}{n} \tag{10}$$

where n represents QOSTBC's dimension or size. In a large number of antennas, orthogonality is close to 0.5, which is the MIMO system's minimum requirement. Therefore, it already fulfill the requirements of the common MIMO systems [26]–[32].

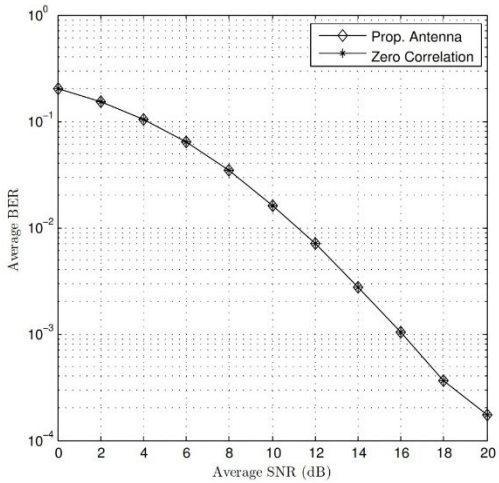

Fig. 9. Average BER of the proposed antenna compared to zero correlation

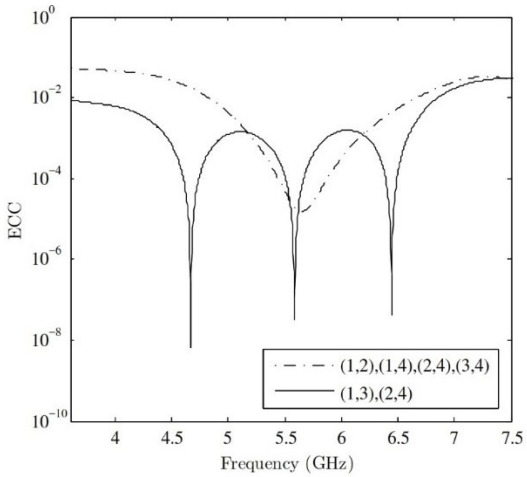

Fig. 10. The obtained ECC of the array antenna

3.2. Beamforming Performance

An array antenna is fed with a phase variation. Back lobe suppression is achieved by setting 90° phase differences between the main and back lobe directions [72]. Table 2 lists the experimental scenario. For example, Fig. 11 shows the effect of phase difference. It has been demonstrated that a 30° phase difference can shift the antenna's main lobe. Another consequence of the phase difference is an enlarged sidelobe. This side effect also reduced the size of the main lobe. The results of the experiment in Table 2 are shown in Fig. 12. It has been confirmed that applied phase difference shifts the main lobe direction by 0.1833° per $\Delta\theta$. The

magnitude of the main lobe decreases as s increases. It is a side effect of phase array beamforming, as previously shown in Fig 10.

Table 2. Phase Configuration of Beamforming Antenna in Fig. 4

$\Delta\theta(°)$	$\theta_1(°)$	$\theta_2(°)$	$\theta_3(°)$	$\theta_4(°)$
0	0	0	-90	-90
15	0	15	-75	-90
30	0	30	-60	-90
45	0	45	-45	-90
60	0	60	-40	-90

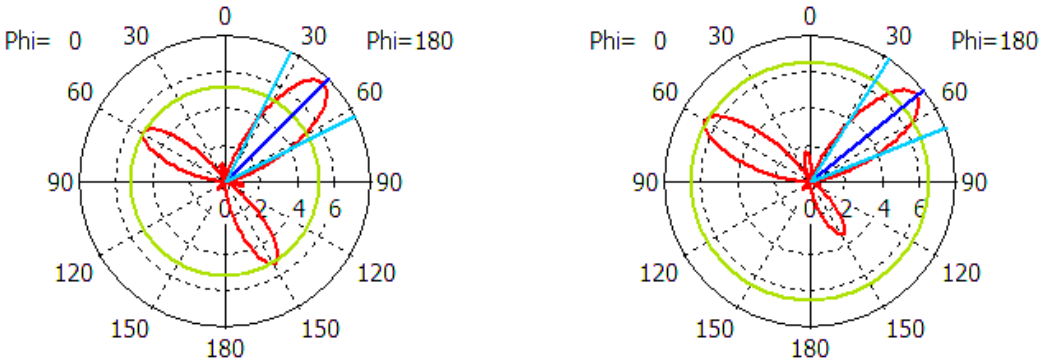

(a) (b)

Fig. 11. Array antenna's radiation pattern: (a) 0° phase difference, (b) 30° phase difference

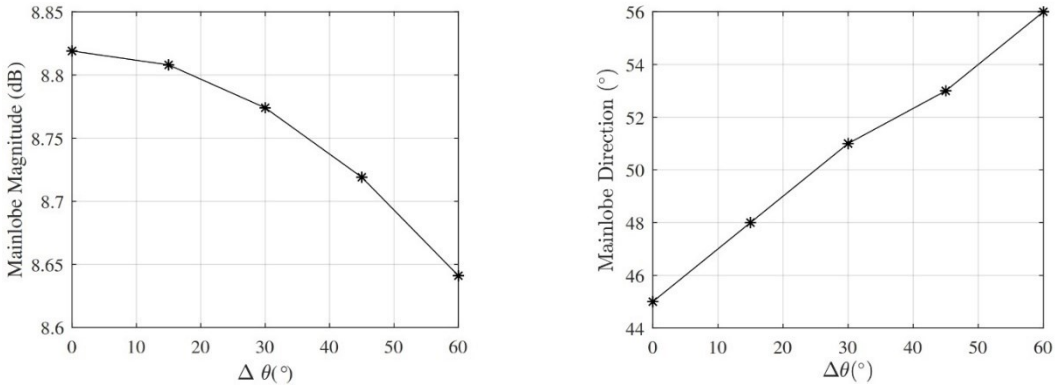

(a) (b)

Fig. 12. Main lobe of antenna from Table 2: (a) magnitude, (b) direction

4. CONCLUSIONS

A four-element dual-mode array of planar dipole antenna for mobile robot communications at 5.6 GHz has been proposed. The proposed antenna can support both beamforming and MIMO. The beamforming of the proposed antenna reaches a gain above 8.6 dBi. The MIMO performance of the proposed antenna is very close to the non-correlated MIMO antenna indicating a very low correlation of the proposed antenna on MIMO mode. The ECC of the proposed antenna is below 0.01.

REFERENCES

[1] D. B. Camarillo, T. M. Krummel, and J. K. Salisbury, "Robotic technology in surgery: Past, present, and future," *Am. J. Surg.*, vol. 188, no. 4, pp. 2–15, Oct. 2004, https://doi.org/10.1016/J.AMJSURG.2004.08.025.

[2] A. Fishman, C. Paxton, W. Yang, D. Fox, B. Boots, and N. Ratliff, "Collaborative interaction models for optimized human-robot teamwork," *IEEE Int. Conf. Intell. Robot. Syst.*, pp. 11221–11228, Oct. 2020, https://doi.org/10.1109/IROS45743.2020.9341369.

[3] M. B. Alatise and G. P. Hancke, "A Review on Challenges of Autonomous Mobile Robot and Sensor Fusion Methods," *IEEE Access*, vol. 8, pp. 39830–39846, 2020, https://doi.org/10.1109/ACCESS.2020.2975643.

[4] L. Romeo, A. Petitti, R. Marani, and A. Milella, "Internet of Robotic Things in Smart Domains: Applications and Challenges," *Sensors 2020,* vol. 20, no. 12, p. 3355, Jun. 2020, https://doi.org/10.3390/S20123355.

[5] M. Z. Miskin *et al.*, "Electronically integrated, mass-manufactured, microscopic robots," *Nat. 2020 5847822*, vol. 584, no. 7822, pp. 557–561, Aug. 2020, https://doi.org/10.1038/s41586-020-2626-9.
[6] M. Gharbia, A. Chang-Richards, Y. Lu, R. Y. Zhong, and H. Li, "Robotic technologies for on-site building construction: A systematic review," *J. Build. Eng.*, vol. 32, p. 101584, Nov. 2020, https://doi.org/10.1016/J.JOBE.2020.101584.
[7] Z. Makhataeva and H. A. Varol, "Augmented Reality for Robotics: A Review," *Robot. 2020, Vol. 9, Page 21*, vol. 9, no. 2, p. 21, Apr. 2020, https://doi.org/10.3390/robotics9020021.
[8] H. J. Lee *et al.*, "Importance of a 5G Network for Construction Sites: Limitation of WLAN in 3D Sensing Applications," *Proceedings of the International Symposium on Automation and Robotics in Construction*, vol. 39, pp. 391-398, 2022, https://www.proquest.com/openview/396c2e0a2d82b7d92916c136743dc096/1?pq-origsite=gscholar&cbl=1646340.
[9] A. Zhou *et al.*, "Robotic Millimeter-Wave Wireless Networks," *IEEE/ACM Trans. Netw.*, vol. 28, no. 4, pp. 1534–1549, Aug. 2020, https://doi.org/10.1109/TNET.2020.2990498.
[10] M. Niihara *et al.*, "A Transportation Routing Method Based on A* Algorithm and Hill Climbing for Swarm Robots in WLAN Environment," *Lect. Notes Networks Syst.*, vol. 570 LNNS, pp. 361–368, 2023, https://doi.org/10.1007/978-3-031-20029-8_35.
[11] M. A. Qasim, F. Abrar, S. Ahmad, and M. Usman, "AI-Based Smart Robot for Restaurant Serving Applications," *Lect. Notes Data Eng. Commun. Technol.*, vol. 105, pp. 107–123, 2022, https://doi.org/10.1007/978-3-030-90618-4_5.
[12] Z. Hou, Y. Pan, J. Xiong, Y. Zeng, and C. Shen, "A frequency reconfigurable antenna for intelligent mobile robot," *13th Int. Conf. Adv. Comput. Intell. ICACI 2021*, pp. 107–111, May 2021, https://doi.org/10.1109/ICACI52617.2021.9435896.
[13] A. A. M. Rahman *et al.*, "Triple band frequency tunable polarization insensitive metamaterial absorber for WLAN and 5G applications," *Opt. Mater. (Amst).*, vol. 145, p. 114368, Nov. 2023, https://doi.org/10.1016/J.OPTMAT.2023.114368.
[14] R. N. Tiwari, R. Thirumalaiah, V. R. Naidu, G. Sreenivasulu, P. Singh, and S. Rajasekaran, "Compact dual band 4-port MIMO antenna for 5G-sub 6 GHz/N38/N41/N90 and WLAN frequency bands," *AEU - Int. J. Electron. Commun.*, vol. 171, p. 154919, Nov. 2023, https://doi.org/10.1016/J.AEUE.2023.154919.
[15] X. Yang *et al.*, "An Integrated Tri-Band Antenna System with Large Frequency Ratio for WLAN and WiGig Applications," *IEEE Trans. Ind. Electron.*, vol. 68, no. 5, pp. 4529–4540, May 2021, https://doi.org/10.1109/TIE.2020.2987289.
[16] P. P. Singh, P. K. Goswami, S. K. Sharma, and G. Goswami, "Frequency reconfigurable multiband antenna for IoT applications in WLAN, Wi-max, and C-band," *Prog. Electromagn. Res. C*, vol. 102, pp. 149–162, 2020, https://doi.org/10.2528/PIERC20022503.
[17] A. T. Al-Heety, M. T. Islam, A. H. Rashid, H. N. A. Ali, A. M. Fadil, and F. Arabian, "Performance evaluation of wireless data traffic in mm wave massive MIMO communication," *Indones. J. Electr. Eng. Comput. Sci.*, vol. 20, no. 3, pp. 1342–1350, 2020, https://doi.org/10.11591/ijeecs.v20.i3.pp1342-1350.
[18] N. Jaglan, S. D. Gupta, and M. S. Sharawi, "18 Element Massive MIMO/Diversity 5G Smartphones Antenna Design for Sub-6 GHz LTE Bands 42/43 Applications," *IEEE Open J. Antennas Propag.*, vol. 2, pp. 533–545, 2021, https://doi.org/10.1109/OJAP.2021.3074290.
[19] M. S. Khan, A. Iftikhar, R. M. Shubair, A. D. Capobianco, B. D. Braaten, and D. E. Anagnostou, "Eight-Element Compact UWB-MIMO/Diversity Antenna with WLAN Band Rejection for 3G/4G/5G Communications," *IEEE Open J. Antennas Propag.*, vol. 1, no. 1, pp. 196–206, 2020, https://doi.org/10.1109/OJAP.2020.2991522.
[20] A. Birwal, S. Singh, B. K. Kanaujia, and S. Kumar, "Low-profile 2.4/5.8 GHz MIMO/diversity antenna for WLAN applications," *J. Electromagn. Waves Appl.*, vol. 34, no. 9, pp. 1283–1299, Jun. 2020, https://doi.org/10.1080/09205071.2020.1757516.
[21] Y. Aslan, A. Roederer, N. J. G. Fonseca, P. Angeletti, and A. Yarovoy, "Orthogonal Versus Zero-Forced Beamforming in Multibeam Antenna Systems: Review and Challenges for Future Wireless Networks," *IEEE J. Microwaves*, vol. 1, no. 4, pp. 879–901, Oct. 2021, https://doi.org/10.1109/JMW.2021.3109244.
[22] Z. D. Zaharis, I. P. Gravas, P. I. Lazaridis, T. V. Yioultsis, C. S. Antonopoulos, and T. D. Xenos, "An Effective Modification of Conventional Beamforming Methods Suitable for Realistic Linear Antenna Arrays," *IEEE Trans. Antennas Propag.*, vol. 68, no. 7, pp. 5269–5279, Jul. 2020, https://doi.org/10.1109/TAP.2020.2977822.
[23] W. Hong *et al.*, "MmWave 5G NR Cellular Handset Prototype Featuring Optically Invisible Beamforming Antenna-on-Display," *IEEE Commun. Mag.*, vol. 58, no. 8, pp. 54–60, Aug. 2020, https://doi.org/10.1109/MCOM.001.2000115.
[24] L. Rao, M. Pant, L. Malviya, A. Parmar, and S. V. Charhate, "5G beamforming techniques for the coverage of intended directions in modern wireless communication: in-depth review," *Int. J. Microw. Wirel. Technol.*, vol. 13, no. 10, pp. 1039–1062, Dec. 2021, https://doi.org/10.1017/S1759078720001622.
[25] Y. J. Guo, M. Ansari, and N. J. G. Fonseca, "Circuit Type Multiple Beamforming Networks for Antenna Arrays in 5G and 6G Terrestrial and Non-Terrestrial Networks," *IEEE J. Microwaves*, vol. 1, no. 3, pp. 704–722, Jul. 2021, https://doi.org/10.1109/JMW.2021.3072873.
[26] M. N. Ashraf, M. U. Khan, T. Hassan, R. Hussain, and M. S. Sharawi, "Reduction of Correlation Coefficient Using Frequency Selective Surface for Multi-band MIMO Antenna," *15th Eur. Conf. Antennas Propagation, EuCAP 2021*, Mar. 2021, https://doi.org/10.23919/EUCAP51087.2021.9411257.

[27] W. Naktong and A. Ruengwaree, "Four-port rectangular monopole antenna for UWB-MIMO," *Prog. Electromagn. Res. B*, vol. 87, pp. 19–38, 2020, https://doi.org/10.2528/PIERB19102902.
[28] X. Mei and K. L. Wu, "Envelope Correlation Coefficient for Multiple MIMO Antennas of Mobile Terminals," *2020 IEEE Int. Symp. Antennas Propag. North Am. Radio Sci. Meet. IEEECONF - Proc.*, pp. 1597–1598, Jul. 2020, https://doi.org/10.1109/IEEECONF35879.2020.9329678.
[29] T. Svantesson, "Correlation and channel capacity of MIMO systems employing multimode antennas," *IEEE Trans. Veh. Technol.*, vol. 51, no. 6, pp. 1304–1312, Nov. 2002, https://doi.org/10.1109/TVT.2002.804856.
[30] N. Honma and K. Murata, "Correlation in MIMO Antennas," *Electron.,* vol. 9, no. 4, p. 651, Apr. 2020, https://doi.org/10.3390/ELECTRONICS9040651.
[31] Y. Liu, X. Yang, Y. Jia, and Y. J. Guo, "A Low Correlation and Mutual Coupling MIMO Antenna," *IEEE Access*, vol. 7, pp. 127384–127392, 2019, https://doi.org/10.1109/ACCESS.2019.2939270.
[32] M. S. Sharawi, A. T. Hassan, and M. U. Khan, "Correlation coefficient calculations for MIMO antenna systems: a comparative study," *Int. J. Microw. Wirel. Technol.*, vol. 9, no. 10, pp. 1991–2004, Dec. 2017, https://doi.org/10.1017/S1759078717000903.
[33] B. J. Niu and Y. J. Cao, "Bandwidth-enhanced four-antenna MIMO system based on SIW cavity," *Electron. Lett.*, vol. 56, no. 13, pp. 643–645, Jun. 2020, https://doi.org/10.1049/EL.2020.0799.
[34] B. Cheng and Z. Du, "A Wideband Low-Profile Microstrip MIMO Antenna for 5G Mobile Phones," *IEEE Trans. Antennas Propag.*, vol. 70, no. 2, pp. 1476–1481, Feb. 2022, https://doi.org/10.1109/TAP.2021.3111330.
[35] A. Ahmad, D. you Choi, and S. Ullah, "A compact two elements MIMO antenna for 5G communication," *Sci. Reports 2022 121*, vol. 12, no. 1, pp. 1–8, Mar. 2022, https://doi.org/10.1038/s41598-022-07579-5.
[36] N. O. Parchin, Y. I. A. Al-Yasir, H. J. Basherlou, and R. A. Abd-Alhameed, "A closely spaced dual-band MIMO patch antenna with reduced mutual coupling for 4G/5G applications," *Prog. Electromagn. Res. C*, vol. 101, pp. 71–80, 2020, https://doi.org/10.2528/PIERC20013001.
[37] I. Elfergani *et al.*, "Low-Profile and Closely Spaced Four-Element MIMO Antenna for Wireless Body Area Networks," *Electron.*, vol. 9, no. 2, p. 258, Feb. 2020, https://doi.org/10.3390/ELECTRONICS9020258.
[38] T. Addepalli and V. R. Anitha, "A very compact and closely spaced circular shaped UWB MIMO antenna with improved isolation," *AEU - Int. J. Electron. Commun.*, vol. 114, p. 153016, Feb. 2020, https://doi.org/10.1016/J.AEUE.2019.153016.
[39] M. Abdullah and S. Koziel, "A novel versatile decoupling structure and expedited inverse-model-based re-design procedure for compact single-and dual-band MIMO antennas," *IEEE Access*, vol. 9, pp. 37656–37667, 2021, https://doi.org/10.1109/ACCESS.2021.3063728.
[40] Y. Qin, R. Li, and Y. Cui, "Embeddable structure for reducing mutual coupling in massive MIMO antennas," *IEEE Access*, vol. 8, pp. 195102–195112, 2020, https://doi.org/10.1109/ACCESS.2020.3033717.
[41] T. Pei, L. Zhu, J. Wang, and W. Wu, "A low-profile decoupling structure for mutual coupling suppression in mimo patch antenna," *IEEE Trans. Antennas Propag.*, vol. 69, no. 10, pp. 6145–6153, Oct. 2021, https://doi.org/10.1109/TAP.2021.3098565.
[42] H. H. Tran, N. Hussain, H. C. Park, and N. Nguyen-Trong, "Isolation in Dual-Sense CP MIMO Antennas and Role of Decoupling Structures," *IEEE Antennas Wirel. Propag. Lett.*, vol. 21, no. 6, pp. 1203–1207, Jun. 2022, https://doi.org/10.1109/LAWP.2022.3161669.
[43] C. Yu *et al.*, "A Super-Wideband and High Isolation MIMO Antenna System Using a Windmill-Shaped Decoupling Structure," *IEEE Access*, vol. 8, pp. 115767–115777, 2020, https://doi.org/10.1109/ACCESS.2020.3004396.
[44] A. Iqbal, A. Altaf, M. Abdullah, M. Alibakhshikenari, E. Limiti, and S. Kim, "Modified U-Shaped Resonator as Decoupling Structure in MIMO Antenna," *Electron.*, vol. 9, no. 8, p. 1321, Aug. 2020, https://doi.org/10.3390/ELECTRONICS9081321.
[45] S. Sharma, Mainuddin, B. K. Kanaujia, and M. K. Khandelwal, "Implementation of four-port MIMO diversity microstrip antenna with suppressed mutual coupling and cross-polarized radiations," *Microsyst. Technol.*, vol. 26, no. 3, pp. 993–1000, Mar. 2020, https://doi.org/10.1007/S00542-019-04574-1/METRICS.
[46] F. Liu, J. Guo, L. Zhao, G. L. Huang, Y. Li, and Y. Yin, "Ceramic Superstrate-Based Decoupling Method for Two Closely Packed Antennas with Cross-Polarization Suppression," *IEEE Trans. Antennas Propag.*, vol. 69, no. 3, pp. 1751–1756, Mar. 2021, https://doi.org/10.1109/TAP.2020.3016388.
[47] H. Hamlbar Gerami, R. Kazemi, and A. E. Fathy, "Development of a metasurface-based slot antenna for 5G MIMO applications with minimized cross-polarization and stable radiation patterns through mode manipulation," *Sci. Reports 2024 141*, vol. 14, no. 1, pp. 1–18, Apr. 2024, https://doi.org/10.1038/s41598-024-58794-1.
[48] B. Feng, T. Luo, T. Zhou, and C. Y. D. Sim, "A dual-polarized antenna with low cross polarization, high gain, and isolation for the fifth-generation array/multiple-input multiple-output communications," *Int. J. RF Microw. Comput. Eng.*, vol. 31, no. 2, p. e22278, Feb. 2021, https://doi.org/10.1002/MMCE.22278.
[49] Muhsin and R. P. Astuti, "Dual-Cross-Polarized Antenna Decoupling for 43 GHz Planar Massive MIMO in Full Duplex Single Channel Communications," *Int. J. Adv. Comput. Sci. Appl.*, vol. 10, no. 4, pp. 364–370, 2019, https://doi.org/10.14569/IJACSA.2019.0100444.
[50] M. Muhsin, A. L. Nurlaili, A. Saharani, and I. R. Utami, "Sectoral dual-polarized MIMO antenna for 5G-NR band N77 base station," *Indones. J. Electr. Eng. Comput. Sci.*, vol. 21, no. 3, pp. 1611–1621, Mar. 2021, https://doi.org/10.11591/ijeecs.v21i3.pp1611-1621.
[51] Z. Zheng, T. Yang, W. Q. Wang, and S. Zhang, "Robust adaptive beamforming via coprime coarray interpolation," *Signal Processing*, vol. 169, p. 107382, Apr. 2020, https://doi.org/10.1016/J.SIGPRO.2019.107382.
[52] I. Mallioras, Z. D. Zaharis, P. I. Lazaridis, and S. Pantelopoulos, "A Novel Realistic Approach of Adaptive

Beamforming Based on Deep Neural Networks," *IEEE Trans. Antennas Propag.*, vol. 70, no. 10, pp. 8833–8848, Oct. 2022, https://doi.org/10.1109/TAP.2022.3168708.
[53] F. Sohrabi, Z. Chen, and W. Yu, "Deep Active Learning Approach to Adaptive Beamforming for mmWave Initial Alignment," *IEEE J. Sel. Areas Commun.*, vol. 39, no. 8, pp. 2347–2360, Aug. 2021, https://doi.org/10.1109/JSAC.2021.3087234.
[54] K. E. Kolodziej, J. P. Doane, B. T. Perry, and J. S. Herd, "Adaptive Beamforming for Multi-Function In-Band Full-Duplex Applications," *IEEE Wirel. Commun.*, vol. 28, no. 1, pp. 28–35, Feb. 2021, https://doi.org/10.1109/MWC.001.2000203.
[55] X. Pei *et al.*, "RIS-Aided Wireless Communications: Prototyping, Adaptive Beamforming, and Indoor/Outdoor Field Trials," *IEEE Trans. Commun.*, vol. 69, no. 12, pp. 8627–8640, Dec. 2021, https://doi.org/10.1109/TCOMM.2021.3116151.
[56] C. Wang *et al.*, "Space Phased Array Antenna Developments: A Perspective on Structural Design," *IEEE Aerosp. Electron. Syst. Mag.*, vol. 35, no. 7, pp. 44–63, Jul. 2020, https://doi.org/10.1109/MAES.2020.2984300.
[57] G. He, X. Gao, L. Sun, and R. Zhang, "A review of multibeam phased array antennas as LEO satellite constellation ground station," *IEEE Access*, vol. 9, pp. 147142–147154, 2021, https://doi.org/10.1109/ACCESS.2021.3124318.
[58] A. K. Vallappil, M. K. A. Rahim, B. A. Khawaja, N. A. Murad, and M. G. Mustapha, "Butler Matrix Based Beamforming Networks For Phased Array Antenna Systems: A Comprehensive Review and Future Directions For 5G Applications," *IEEE Access*, vol. 9, pp. 3970–3987, 2021, https://doi.org/10.1109/ACCESS.2020.3047696.
[59] G. Yang, Y. Zhang, and S. Zhang, "Wide-Band and Wide-Angle Scanning Phased Array Antenna for Mobile Communication System," *IEEE Open J. Antennas Propag.*, vol. 2, pp. 203–212, 2021, https://doi.org/10.1109/OJAP.2021.3057062.
[60] G. Yang and S. Zhang, "Dual-Polarized Wide-Angle Scanning Phased Array Antenna for 5G Communication Systems," *IEEE Trans. Antennas Propag.*, vol. 70, no. 9, pp. 7427–7438, Sep. 2022, https://doi.org/10.1109/TAP.2022.3141188.
[61] H. Al Kassir, Z. D. Zaharis, P. I. Lazaridis, N. V. Kantartzis, T. V. Yioultsis, and T. D. Xenos, "A Review of the State of the Art and Future Challenges of Deep Learning-Based Beamforming," *IEEE Access*, vol. 10, pp. 80869–80882, 2022, https://doi.org/10.1109/ACCESS.2022.3195299.
[62] B. Jalal, X. Yang, Q. Liu, T. Long, and T. K. Sarkar, "Fast and Robust Variable-Step-Size LMS Algorithm for Adaptive Beamforming," *IEEE Antennas Wirel. Propag. Lett.*, vol. 19, no. 7, pp. 1206–1210, Jul. 2020, https://doi.org/10.1109/LAWP.2020.2995244.
[63] E. E. Bahingayi and K. Lee, "Low-Complexity Beamforming Algorithms for IRS-Aided Single-User Massive MIMO mmWave Systems," *IEEE Trans. Wirel. Commun.*, vol. 21, no. 11, pp. 9200–9211, Nov. 2022, https://doi.org/10.1109/TWC.2022.3174154.
[64] M. Abualhayja'a and M. Hussein, "Comparative Study of Adaptive Beamforming Algorithms for Smart antenna Applications," *ICCSPA 4th Int. Conf. Commun. Signal Process. their Appl.*, pp. 1-5, Mar. 2021, https://doi.org/10.1109/ICCSPA49915.2021.9385725.
[65] N. Ramli, S. K. Noor, T. Khalifa, and N. H. Abd Rahman, "Design and Performance Analysis of Different Dielectric Substrate based Microstrip Patch Antenna for 5G Applications," *Int. J. Adv. Comput. Sci. Appl.*, vol. 11, no. 8, pp. 77–83, 2020, https://doi.org/10.14569/IJACSA.2020.0110811.
[66] H. Jafarkhani, "A quasi-orthogonal space-time block code," *IEEE Trans. Commun.*, vol. 49, no. 1, pp. 1–4, 2001, https://doi.org/10.1109/26.898239.
[67] E. A. Jorswieck and H. Boche, "Channel capacity and capacity-range of beamforming in MIMO wireless systems under correlated fading with covariance feedback," *IEEE Trans. Wirel. Commun.*, vol. 3, no. 5, pp. 1543–1553, Sep. 2004, https://doi.org/10.1109/TWC.2004.833523.
[68] Muhsin and K. Anwar, "ABBA Dual-Cross-Polarized Antenna Decoupling for 5G 16-Element Planar MIMO at 28 GHz," *2nd Int. Conf. Telemat. Futur. Gener. Networks, TAFGEN 2018*, pp. 1–6, Dec. 2018, https://doi.org/10.1109/TAFGEN.2018.8580475.
[69] M. Muhsin, W. M. Hadiansyah, A. P. Pramita, and R. D. N. Cahyanti, "Planar dipole MIMO array antenna for mobile robot communications at 5.6 GHz," *4th Int. Conf. Inf. Technol. Inf. Syst. Electr. Eng. ICITISEE 2019*, pp. 244–248, Nov. 2019, https://doi.org/10.1109/ICITISEE48480.2019.9003753.
[70] A. A. Glazunov, "Mean effective gain of user equipment antennas in double directional channels," *IEEE Int. Symp. Pers. Indoor Mob. Radio Commun. PIMRC*, vol. 1, pp. 432–436, 2004, https://doi.org/10.1109/PIMRC.2004.1370908.
[71] S. Blanch, J. Romeu, and I. Corbella, "Exact representation of antenna system diversity performance from input parameter description," *Electron. Lett.*, vol. 39, no. 9, pp. 705–707, May 2003, https://doi.org/10.1049/EL:20030495.
[72] M. Muhsin, W. M. Hadiansyah, A. Saharani, I. R. Utami, and P. D. Srihadi, "Planar Dipole Array Antenna Design for Mobile Robot Communications at 5.6 GHz," *J. Phys. Conf. Ser.*, vol. 1501, no. 1, p. 012008, Mar. 2020, https://doi.org/10.1088/1742-6596/1501/1/012008.